Potential Surfaces and Dynamics of Weakly Bound Trimers: Perspectives from High Resolution IR Spectroscopy

Martin A. Suhm
Laboratorium für Physikalische Chemie der ETH Zürich (Zentrum), CH-8092 Zürich, Switzerland
David J. Nesbitt*
Department of Chemistry and Biochemistry, University of Colorado, and Joint Institute for Laboratory Astrophysics, University of Colorado and National Institute of Standards and Technology, Boulder, Colorado 80309-0440, U.S.A.

1 Introduction

If we want to understand the properties of condensed molecular matter in detail, we have to study the interactions *between* molecules, which are often summarized under the name 'van der Waals interactions.' These *inter*molecular interactions are of a profoundly subtle, multidimensional, long-range, and coupled nature. This is in contrast to *intra*molecular interactions, where the concepts of chemical bond and harmonic force-field usually form a reasonably localized zero-order reference point at sufficiently low excitation levels. Infrared spectroscopy provides a powerful general tool to study both inter- and intramolecular interactions, since it can cover the full frequency range of fundamental and few-quantum excitation of the associated degrees of freedom. It is in the 'floppy molecule', intermolecular regime where the inversion of high resolution spectroscopic data to interaction potentials is particularly difficult, and thus the demand for interaction between theory and experiment is particularly intense.

As one consequence of this difficulty, initial spectroscopic research efforts have concentrated on *pairs* of molecules, the obvious prototypes of any interaction study. These binary complexes or dimers[1] have revealed an unprecedented richness of structural properties and dynamical behaviour, when viewed through the eyes of high resolution microwave, far- and near-IR spectroscopy,[2-5] and modern theoretical tools. Indeed, the astonishing range of challenges and insights provided by *dimer* spectroscopy deflected the original thrust of a spectroscopy-based understanding of *bulk* matter toward an extensive, albeit very fruitful, series of diversions. The reader might compare this to the situation of a sociologist heading out for a systematic understanding of human interactions in large groups, who finds himself stuck at the level of pairwise interactions due to the enormous wealth of insights to be gained in this simplest of all social groups.

With more than a decade of theoretical and experimental effort in studies of dimers, the investigation of larger clusters is now beginning to be tractable at high resolution. Occam's razor suggests a pragmatic starting point. The interactions of a large ensemble of molecules (or human beings, to play the analogy a little further) are most simply described as the *sum* over all possible pair interactions. However, it is also immediately clear (both in spectroscopy and in sociology) that this is only an *approximation* to the true nature of molecular forces. The *extent* of approximation inherent in the so-called 'pairwise additive' approach varies from system to system; consequently its detailed experimental characterization in weakly bound systems is both a necessary and challenging step.

The obvious prototype for the study of non-pairwise additivity are molecular trimers[1] *i.e.*, the simplest systems wherein three-body forces are superimposed on the pairwise forces. These three-body forces and their associated multidimensional potentials are defined by the property that they vanish when any one of the three units is separated from the others. To extract them from the full interaction potential, the pairwise interactions have to be accurately known, as the non-pairwise additivity is typically a relatively small fraction of the pair interactions. This explains in part the reluctance with which trimers have been previously investigated by spectroscopy and theory, but we are now rapidly approaching a point where many important systems have become eligible for in-depth analysis.

Rather than even attempting a literature survey of systems investigated, we concentrate in this review on the homologous series of trimers composed of Ar and HF[1] (see also Figure 1):

$$(HF)_3 \rightarrow Ar(HF)_2 \rightarrow Ar_2HF \rightarrow Ar_3 \qquad (1)$$

* Staff member, Quantum Physics Division, National Institute of Standards and Technology.

Martin Suhm (b.1962) grew up in Germany and Portugal. He studied chemistry at the University of Karlsruhe, obtaining a diploma thesis under Professor H. G. Hertz in 1985. After a research year with Professor R. O. Watts at the Australian National University in Canberra (1986), he joined Professor M. Quack's group at ETH Zürich (Ph.D., 1990). Since then, he has worked towards a detailed experimental and theoretical understanding of larger HF clusters, at ETH Zürich and for several months with Professor D. J. Nesbitt's group at JILA in Boulder (1990–1992). His research interests concentrate on three-body and quantum effects in intermolecular interactions.

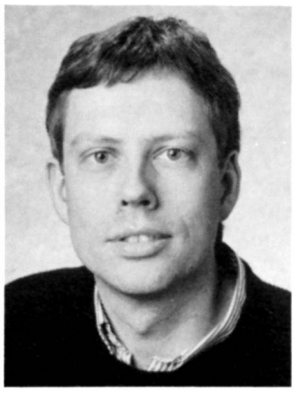

David Nesbitt did his undergraduate studies in physics and chemistry at Harvard University, and then taught secondary school science and maths for two years, prior to entering the Ph.D. programme in chemical physics at the University of Colorado, Boulder. Following his Ph.D. work, Nesbitt pursued a Miller Fellowship at the University of California, Berkeley where he developed methods for high sensitivity tunable IR detection of ions and radicals. He is presently a Professor Adjoint in the Department of Chemistry and Biochemistry at the University of Colorado, and Fellow of the Joint Institute for Laboratory Astrophysics, through the National Institute of Standards and Technology.

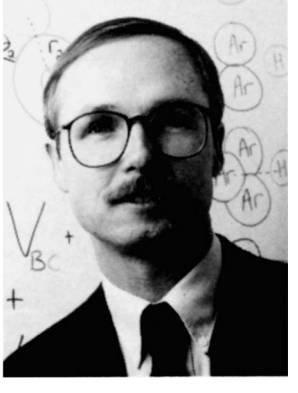

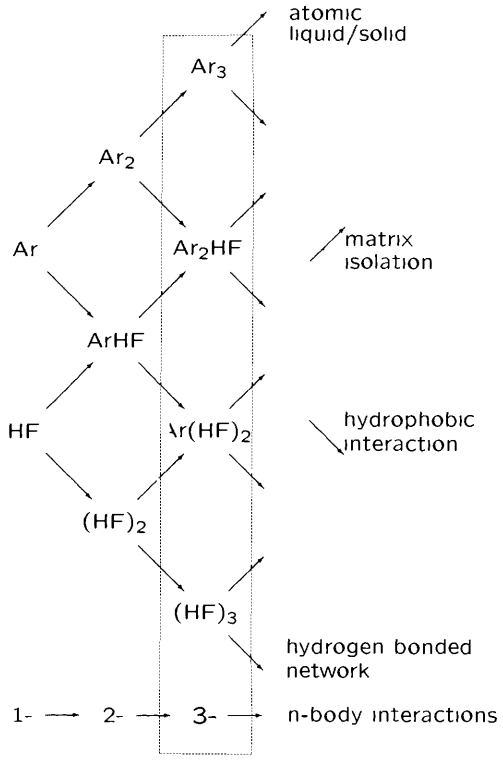

Figure 1 Trimers and three-body forces on the path toward understanding bulk phases The molecular monomer (HF) is described by a one-body potential Interaction between monomers of the same kind leads to homo-dimers [$(HF)_2$ and Ar_2], which are fully described by pairwise (two-body) interactions In a first approximation, oligomers of any size and the condensed Ar and HF phases can be described as the sum over all possible pairwise interactions Additional knowledge of the Ar–HF pair potential from the study of ArHF allows a pairwise additive description of all mixed clusters and phases, including the limit of an Ar atom solvated by HF (a model for hydrophobic interaction) and that of a HF molecule embedded in an Ar matrix Investigation of trimers makes it possible to judge the quality of pairwise interaction models It is found that hydrogen-bonded networks are strongly affected by three-body contributions, whereas the effects are smaller for rare gas and rare gas–polar molecule interactions

This series contains some of the best understood trimers and also some less studied ones More importantly, the series spans a comprehensive range of *types* of intermolecular interactions, and hence *types* of three-body interactions, ranging from strong hydrogen bonding to electrostatic and polarization interactions, to the weak, purely quantum dispersion forces As illustrated in Figure 1, the series provides a simple touchstone for various classes of condensed matter, ranging from hydrogen-bonded networks and hydrophobic interactions, which are at the heart of many biological and chemical phenomena, to simple liquids and solids, including also simple solute–solvent and solid matrix embedding interactions

2 Intermolecular Interactions

2.1 A Loose Classification

Before dealing with IR spectroscopy as a probe of potential energy surfaces, we must first introduce some basic concepts of intermolecular interactions We will do this in an informal, illustrative way, a more detailed, mathematical, and systematic treatment would be beyond the scope of this article and excellent accounts can be found in other places [6 8]

Electrostatic interactions between molecules are those which arise from the static electric moments (charges, dipoles, quadrupoles) of the *isolated* molecules, possibly dependent on the internal state or distortion of the molecular units These interactions are described by the well-known (pairwise) Coulomb law and leave no room for any non-additive, *e g* three-body, effects

Induction forces arise from the interaction of electrostatic moments on one molecule with the polarizable electron cloud of the other For instance, a dipolar molecule *A* (such as HF) interacts with a polarizable molecule *B* and induces a dipole in this molecule (or increases an existing one) This, in turn, increases the dipole of *A* somewhat, if *A* also happens to be polarizable Addition of a third molecule *C* offers new options in this chain interaction *A* polarizes *B*, *B* polarizes *C*, *C* polarizes *A*, and the polarization acts back on the molecules inducing them By closing the polarization chain to a *ring*, the effect is maximized The equilateral triangle is thus a favourable arrangement for this kind of interaction Obviously, the full polarization effect is not equal to the sum of the *AB*, *BC*, and *AC* effects, but will contain a three-body term *ABC* depending on the positions of all three molecules simultaneously This is an important source for non-additive interactions in polar systems

Dispersion interaction is a quantum effect which is somewhat more difficult to visualize Imagine *A* and *B* to be polarizable, but without permanent (dipole) moments to polarize each other (*e g* , rare gas atoms) Then, a long 'Coulombic conversation' goes on between the two For example, if *A* were to achieve some temporary distortion of its election cloud to generate an instantaneous dipole, then *B* would polarize to accommodate and thereby *lower* the total energy Exploring all these possibilities (within the constraints of Heisenberg's uncertainty principle) leads to a mutual dynamic attraction of the molecules, the so called London or dispersion force, which grows with the polarizability of the system It is easy to imagine that this type of interaction will be influenced beyond additivity by a third party *C* Rigorous quantum mechanical treatment yields the so called Axilrod–Teller triple-dipole dispersion term[9] as the leading non-additive contribution at long distances The 'fame' of this term exceeds by far its quantitative importance in this discussion, specifically, it is only dominant when virtually all other three-body mechanisms are absent A little bit of thought suggests that this subtle interaction will be disfavoured by an equilateral triangular configuration of *A*, *B*, and *C*, resulting in a repulsive three-body contribution Of course, the overall dispersion interaction remains attractive, but it is simply less so than for three separate pair interactions added together

The Pauli exclusion principle provides another quantum effect which becomes important when two molecules approach each other closely As the Pauli principle does not allow the electrons of *A* and *B* to be in the same state ('spin-orbital'), *A* and *B* will distort each other's electron cloud and influence each other's properties, *e g* the polarizability A distorted *AB* pair will interact differently with a third molecule *C* than *A* and *B* separately, giving rise to various kinds of three-body contributions While there are simple analytical expressions for the leading terms of dispersion and polarization non-additivities, the Pauli effects are more difficult to write down in closed form On the other hand, they are relatively easy to calculate numerically by *ab initio* techniques, as they are captured to a large extent at the SCF level Ironically, it is often the analytical representations of such non-additive interaction contributions that represent the most significant bottleneck for theoretical treatments

In the series (equation 1) with a highly polar HF and a highly polarizable Ar, induction forces will decrease from left to right, whereas dispersion forces will increase Pauli exclusion is more pronounced for stronger interactions, hence the associated effects are expected to be considerably larger for $(HF)_3$ than for $(Ar)_3$ This applies to two- as well as three-body forces and supports the experimental findings that HF is among the non-ionic systems with most pronounced (and attractive) non-pairwise additivity effects[6 7 10] whereas in Ar such effects are very hard to identify and are the subject of considerable debate [11]

2.2 Modelling of Potential Surfaces

Ultimately, we want to relate the spectroscopy and dynamics of weakly bound complexes to the full $3N-6$ dimensional (ground state) potential surface V, where N is the number of atoms involved This potential surface is defined by the lowest possible electronic energy at a given configuration of clamped nuclei As the task of solving the electronic Schrodinger equation for arbitrarily large numbers of clamped geometries is formidable, one is forced to resort to simplified treatments One way is to solve the electronic problem for a selected number of nuclear configurations and to fit analytical expressions to these points The functional form and parameters are often guided by the different classes of interactions discussed in the preceding sections For accurate fits to the data, very flexible functions have to be introduced, since some contributions to the potential surface have no simple or known functional dependence As a result of the large amount of labour and bias associated with the fitting process, alternative representations, such as regular grids combined with interpolation, have been attempted However, these methods are usually handicapped by unfavourable scaling with dimensionality For example, assuming only 10 grid points per dimension, the total number of grid points is $10^{(3N-6)}$ and hence impractical for more than about four atoms Irregular grids concentrating on the potential surface regions which are relevant for spectroscopy and dynamics are more powerful, but also more difficult to generate and to interpolate This is an area where considerably more work needs to be done Some new ways to work with such irregular potential energy surface samples are described in reference 12

3 IR Spectroscopy

3.1 Spectral Regions and Techniques

The infrared region accesses most of the dynamic range of nuclear vibrational motion present in weakly bound clusters IR spectroscopy is a sensitive probe of the nuclear dynamics whenever the molecular dipole moment is affected by it The fundamental excitations of van der Waals modes fall typically into the far infrared domain ($\lambda \approx 20$–1000μm), which is among the most difficult to access experimentally Incoherent radiation sources used in broad band interferometric spectroscopy (FTIR)[13 14] are weak, although synchrotron radiation may provide an attractive future option Tunable far infrared lasers offer considerably higher resolution,[15] but they are still in a relatively early stage Infrared activity of van der Waals modes can be poor, in particular for stretching fundamentals, which, in the absence of strong mixing of vibrational states, commonly have little effect on the dipole moment Thus, far infrared studies of van der Waals clusters typically require supersonic jet expansions or cells with long optical path lengths The cells have to be coolable[13 16] in order to optimize complexation, while the supersonic expansions are most favourably planar[3 15] to magnify the high density region to be probed in direct absorption The long wavelength suggests wave-guide concepts or build-up cavities could be used to realize extended optical paths At thermal equilibrium, light pipe cells have been used successfully,[14] where the radiation is efficiently guided through a highly conducting metal cell *via* multiple wall reflections An alternative way to solve the problem of weak absorbance is the use of rare gas matrices as hosts for weakly bound complexes at much higher local densities than in the gas phase Despite the lack of rotational structure and potential influence of the matrix, such spectra have contributed importantly to the identification and characterization of strongly bound aggregates [17]

Complementary to the far-IR study of van der Waals or intermolecular vibrations, intermolecular interactions can be studied through combination bands in the mid-to-near infrared, *via* intermolecular bands built on strong intramolecular absorptions of the monomer [4 18] Here, lasers and interferometric spectrometers are both well established and a large number of techniques exists In this range, resolution is typically not limited by laser technology, but rather by Doppler broadening (which can be largely reduced in slit jet expansions[3]) and most importantly by the lifetime of excited states above the cluster dissociation threshold Vibrational *predissociation*, *i e*, the fragmentation of the clusters upon vibrational excitation, can also be exploited for detection in molecular beam techniques by monitoring the laser-induced depletion of the directed flow, either by using a mass spectrometer[19] or a bolometer detector [5]

Trimer species are rarely the dominant clusters in a supersonic expansion or at thermal equilibrium For dominantly isotropic intermolecular interactions, the stability curve as a function of cluster size is rather smooth and one can optimize the trimer concentration by simple dilution [20 21] For anisotropic interactions such as hydrogen bonding, there are different binding patterns Where dimers already achieve reciprocal saturation of their intermolecular valences, such as in carbonic acids, larger aggregates are not favoured at all In many other hydrogen bonding molecules (HF, H_2O, CH_3OH), the donor and acceptor atoms are adjacent This favours ring geometries for medium-sized clusters [19 22 24] For trimers, such rings are severely strained but still favoured over chain-like conformations, because three rather than two intermolecular bonds are formed (see Figure 2) Strain is substantially released from tetramers upwards, typically causing these species to be most stable against monomer vaporization [25]

In a mixture of differently sized clusters, an important issue is cluster identification This is usually not a problem for binary complexes owing to the availability of high-resolution information For larger cluster sizes, ingenious size-selection techniques have been devised [23] Trimers are intermediate, but spectroscopic information is often sufficient for their identification [19 21 24]

3.2 Spectral Information

IR cluster spectra contain structural information on the ground and vibrationally excited states through the rotational constants A, B, C (in decreasing order), which are obtained from an analysis of high-resolution ro-vibrational spectra and are inversely proportional to the corresponding moments of inertia This information is particularly valuable in the absence of a permanent dipole moment for the complex, as in the case of cyclic homo-trimers, where microwave techniques are not applicable The resulting structures are vibrationally averaged, and can differ substantially from the minimum structures obtained from electronic calculations

Infrared-active van der Waals fundamental vibrations provide particularly important information about the shape of the interaction potential For weak interactions, these fundamental vibrations may have sizeable amplitude and they are therefore sensitive to the intermolecular potential surface in a large region They can be classified broadly into two types Stretching modes involve translation of the monomer constituents and can occur for atomic and molecular subunits Librations correspond to hindered rotations of the (molecular) subunits Clearly, the large amplitude often leads to mixing between the two types of motion, but as a zero-order picture, the classification can be useful Compared to binary complexes, which also contain stretching and librational modes, trimers introduce an additional 'twist' Here, the stretching modes can induce a structural change from cyclic to chain-like conformations A new dynamical process – ring opening – can be studied (see Figure 2) [24 26 27]

The infrared active monomer fundamentals in complexes are characteristically shifted from their unperturbed positions [28] While they explore a relatively small section of configuration space, their shifts and intensity changes are powerful probes of the intermolecular interaction Furthermore, predissociation of the excited states can be exquisitely sensitive to the extent of coupling between intra- and intermolecular degrees of freedom, one of the most subtle effects of intermolecular interactions For a trimer, two types of fragmentation pathways or channels are

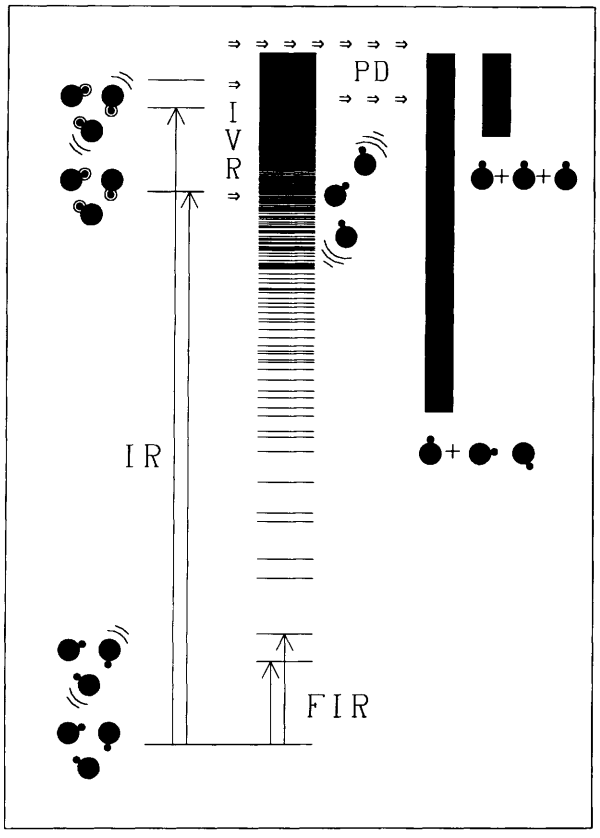

Figure 2 Spectroscopic probes of the dynamics of trimers, exemplified by an $(HX)_3$ trimer energy levels and cartoons of the complex are shown on the left side They are classified into sparse and high-lying intramolecular excitations (left-most, probed by mid-IR spectroscopy, excitation symbolized by a circle around the hydrogen) and intermolecular excitations, which quickly grow in number with increasing energy because of the high dimensionality, finally forming a quasi-continuum The lowest levels are directly accessible by FIR spectroscopy At high energy, most of the intermolecular excitations correspond to open chains (middle) rather than closed rings (left), as the former are favoured by entropy Due to coupling between intramolecular and intermolecular excitation at high energies, intramolecular vibrational redistribution (IVR, arrows) can occur, leading to excess line structure or line broadening in the IR spectrum Above a certain energy, the trimer can fragment into a dimer and a monomer At even higher energies, fragmentation into three monomers becomes feasible Both processes are shown on the right by black bars symbolizing the continuum of states associated with the fragments Predissociation of excited cluster states (PD, arrows) can occur directly or *via* preceeding IVR steps, whenever the energy is above threshold

available (Figure 2) dissociation into three monomers or into a monomer and a dimer The relative abundance of these two types of channels and the detailed mechanisms of energy flow during such processes are among the challenging problems in the field of trimers

Strictly speaking, one would need a time-resolved experiment to determine predissociation lifetimes For isolated transitions, there is however a heavily used spectroscopic shortcut Predissociative decay with a single exponential lifetime τ_{PD} induces a Lorentzian line shape with a full width at half maximum

$$\Delta\nu_{PD} = 1/(2\pi\tau_{PD}) \qquad (2)$$

in the IR spectrum For typical trimers, the requirement of isolated transitions is not always warranted owing to the very large density of states associated with the soft degrees of freedom In such a case, energy flow within the cluster (intramolecular vibrational energy redistribution, IVR) leads to sequential predissociation pathways which compete with direct decay (see Figure 2) and may actually form the bottleneck for the fragmentation process [29]

If vibrational excitation stays *below* the fragmentation threshold, energy flow *within* the cluster is the only process available, and spectroscopy provides information on the speed and pathways for IVR There are two ways to look at these processes From a traditional spectroscopic viewpoint, the excited energy levels are eigenstates which involve a mixture of monomer and van der Waals contributions For the trimers and excitation energies which we discuss here, the density of states is low enough to allow these eigenstates to be resolved (at least in principle), even in the presence of strong coupling According to the defining property of eigenstates, as eigenfunctions of the total Hamiltonian, there is no 'flow' of energy in time, but the character of the excited state can change very rapidly by tuning the excitation frequency An alternative, dynamical viewpoint considers initial excitation of the local *monomer* vibration, which is *not* an eigenstate of the coupled system To achieve such a local excitation, one can use the fact that the monomer coordinate carries most of the dipole oscillator strength By applying a coherent short laser pulse which covers the whole spectral profile of the involved states, the *local* oscillator is initially excited Subsequently, the excitation energy can flow explicitly into the interacting van der Waals modes Under certain conditions,[29] which in particular require a dense manifold of interacting states, this energy flow is exponential in time, it is then analogous to the predissociation process Hence, the spectral profile is again Lorentzian in shape, with a spectral width $\Delta\nu_{IVR}$ related to the lifetime τ_{IVR} *via*

$$\Delta\nu_{IVR} = 1/(2\pi\tau_{IVR}) \qquad (3)$$

Particularly for rapid processes, such a pulsed experiment can be technologically more demanding than simply spectroscopic probing of the eigenstate profile On the other hand, if there are several processes occurring sequentially in time, it can be quite a challenge to extract this dynamical information purely from frequency domain methods However, by applying the relation between lifetime and spectral width (within its range of validity), one can often extract IVR and/or predissociation lifetimes from the spectral profile for the rate limiting process in such a sequence We will discuss such an application for $(DF)_3$

Finally, one can study inter–intramolecular combination bands, resulting from joint excitation of a monomer vibration and a van der Waals degree of freedom (Figure 2) Because of favourable experimental accessibility of widely scanning high resolution light sources in the near-IR, this is often the first information obtained about van der Waals modes [3 21] The results can be combined with far-IR studies or hot bands originating from thermally populated van der Waals states[3 30 31] in order to obtain information on the dependence of *intermolecular* van der Waals modes with *intramolecular* excitation

4 Connecting Potentials with Spectra

When the number of atoms exceeds 3, making the connection between potential energy surfaces and infrared spectra is a highly non-trivial task Figure 3 illustrates some of the aspects involved In a forward strategy, the spectrum for a given (*e g ab initio*) potential surface is predicted and compared to experiment Further iterations may then involve systematic potential surface adjustments to improve agreement [32] More ambitious is the reverse process, *i e* direct inversion of the experimental spectrum to yield a potential surface [8] For all but the simplest systems (*i e* , 1-D), such an inversion is only feasible provided some information about the shape of the potential is available and the experimental data are exhaustive

4.1 Global Connections

Given a potential energy surface, which could be either *ab initio* based or comprised of empirical pair potentials, full ro-vibra-

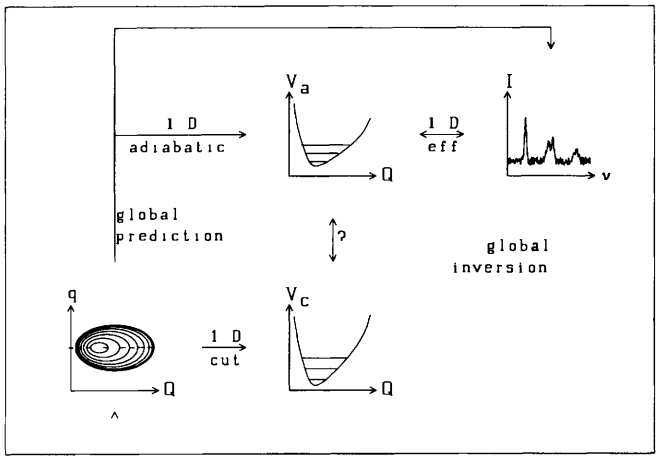

Figure 3 The connection between multidimensional potential surfaces (lower left corner) and IR spectra [upper right corner $I(\nu)$] is based on solutions of the ro vibrational Schrodinger equation Global predictions (large arrow *e g* DQMC) and inversions (dashed arrow) include all degrees of freedom Adiabatic potentials (V_a) describe slow degrees of freedom (Q) but include the *average* effect of the fast ones (q) This is important for anisotropic intermolecular interactions such as hydrogen bonding In the absence of *specific* couplings adiabatic predictions can be compared directly to experimental spectra Simple cuts through the multidimensional potential surface along slow coordinates (V_c) do not capture these average effects and are often not directly comparable to experimental 1 D potentials

tional predictions are well established for up to three atoms and are becoming available for tetratomic systems It is therefore clear that treatments of all but the simplest trimers including all nuclear dimensions are the exception and are usually restricted to some selected states (*e g* by quantum Monte Carlo techniques, see Section 5) or by dynamical approximation [29] Among the most powerful of these is the adiabatic approximation, whereby one attempts to factor the full wavefunction Ψ of the complex into a product of ϕ (the wavefunction of some fast degrees of freedom q) and χ (the wavefunction in the slower coordinates Q) $\phi(q)$ will also generally depend parametrically on the slow coordinates (*i e* $\phi(q,Q)$), but it is assumed to adjust immediately to any change in those $\chi(Q)$, on the other hand, only feels the average effect of $\phi(q,Q)$ The effect of $\phi(q,Q)$ on the slow motion $\chi(Q)$ can therefore be described by an *effective* potential $V_a(Q)$, composed of the true potential energy $V(Q)$ *plus* the instantaneous vibrational energy of ϕ along q Note that this adiabatic separation does not throw away any coordinates The treatment remains global, but it is simplified by identifying and characterizing a set of coordinates In this sense, it is very close to spectroscopic practice, where one tries to assign approximate quantum numbers to observed bands even though the corresponding operators may not commute perfectly with the total Hamiltonian In Section 5 we will discuss some applications for the hydrogen fluoride trimer

4.2 Reduced Dimensionality Connections

Quite often, a reduced subspace of the full potential energy surface is selected and investigated separately The selection requires some insight into the qualitative aspects of the potential surface in order to minimize couplings with other degrees of freedom Reduced subspaces are extremely useful if one wants to model and extrapolate a selected spectroscopic data set They are absolutely crucial in large systems for obtaining physical insight into many dynamical effects

As soon as a subspace of the full configuration space of a complex is selected, the correspondence between forward and inversion strategies breaks down In the forward strategy, one has to make some cut through the full potential (Figure 3), whereas the inversion strategy involves the assignment of quantum numbers to some selection of spectral transitions In both cases, there is some arbitrariness in the coordinate (for the cut and for the quantum numbers), but often there is an obvious choice Furthermore, any specific couplings crossing the subspace boundaries are lost, but of course the weakness of such couplings is a key assumption of any reduced dimensionality treatment For low frequency motions, there is a more serious problem Low frequency motion occurs in the mean field of the faster degrees of freedom (Section 4 1) If these fast degrees of freedom change significantly with the low frequency coordinate, their zero-point energy contribution to the low frequency potential is not constant Hence, the effective low frequency potential as obtained from experiment is already *distorted* with respect to a cut through the full potential surface (Figure 3) This effect is particularly important in hydrogen bonding, as we will see in the example of hydrogen fluoride trimer

With these limitations in mind, there are several options for reduced dimensionality treatments of trimers An obvious simplification is the combined treatment of all intermolecular degrees of freedom, while the monomers are kept at their equilibrium or some vibrationally averaged value [8 33] The justification for this rigid monomer model is the time scale separation of the two types of modes Slow intermolecular motion only sees an average effect of the fast monomer vibrations By studying the van der Waals spectrum as a function of monomer vibrational state, one can extract intermolecular potentials which depend parametrically on the monomer quantum numbers [38] This set of intermolecular potentials for vibrating monomers can then be extrapolated to a potential for vibrationless monomers, which finally represents a true cut through the full potential surface Turning these arguments around, a reasonable first-order description of the *intra*molecular degrees of freedom is often achieved by freezing the soft modes at equilibrium and looking at monomer vibrations in this frozen frame

Within the intermolecular manifold, separation of radial and angular coordinates has been a popular simplification [34] The radial coordinates correspond to distances between monomers and as a consequence, they involve relatively large masses, hence low frequencies Angular coordinates describe internal hindered rotations of the monomers in the framework of the complex For simple hydride rotors such as HF, the moment of inertia is small and the associated librational frequencies are rather high This might suggest that the two subspaces are relatively uncoupled, but the opposite is often true Along the radial monomer separation coordinate, for example, the angular motion changes from nearly vibrational to purely rotational character Vibrations have an associated zero-point energy, whereas rotations do not Therefore, angular–radial separations are at their best when the angular motion is already quite free near the potential energy minimum and only becomes constrained at much shorter separations, *i e* for weak van der Waals bonds [21] For strong hydrogen bond systems, a formal separation may still be possible, but the resulting effective angular and radial potentials do not correspond to simple cuts through the full potential surface (Figure 3)

In any event, the complexity of trimers requires combined efforts along these lines in order to establish the relevant parts of the corresponding multidimensional potential surfaces The power of IR spectroscopy to reveal the properties of these potential energy surfaces varies strongly with the type of molecule and with the type of motion involved This will be illustrated in the following examples

5 $(HF)_3$ and $(DF)_3$ – Not So Weakly Bound Trimers

At the very left of the sequence (equation 1) we have the strongly hydrogen-bonded complex $(HF)_3$ and its isotopomer $(DF)_3$ The equilibrium structure of $(HF)_3$ is planar and cyclic, with C_{3h} symmetry Definite experimental data for this structure were missing until recently,[19 24] although there was early evidence that none of the abundant HF clusters beyond the dimer has an

appreciable dipole moment.[2] This makes a microwave study difficult, as one has to resort to non-symmetric isotopomers such as $(HF)_2DF$ in order to observe a weak, zero-point motion induced dipole moment, and hence rotational spectrum. Thus, we have a classic case where IR spectroscopy provides the first glimpses of structural information even for the ground state. The HF stretching spectra of $(HF)_3$ and some of its isotopomers have been studied at low resolution by monitoring the signal depletion in a mass spectrometer upon IR predissociation[19] and also in rare gas matrices.[17] Although the assignment of the HF stretching bands has gone through some controversial stages, the final result of a detailed study[19] is fully consistent with C_{3h} symmetry, which predicts exactly one IR active (degenerate) HF stretching fundamental in $(HF)_3$. The wavenumber shift relative to HF monomer was found to be $-249\,cm^{-1}$. Compared to the shifts in $(HF)_2$ (-31 and $-93\,cm^{-1}$), this already indicates some sort of non-additivity in the trimer. In fact, the three-body contribution to this shift is $\approx 50\%$ (see Table 1).[35] It is common practice to compare experimentally observed monomer frequency shifts with easily accessible *ab initio harmonic* shift predictions, assuming that intermolecular interaction mainly changes the quadratic force constant of the monomer potential. However, accurate calculations carried out for $(HF)_3$ reveal a 10–20% anharmonicity contribution to the shift in this case.[35]

High resolution investigations of the $(HF)_3$ band do not reveal any rotational structure despite the low temperature in the supersonic expansion. This is in clear contrast to the findings in $(HF)_2$ and shows that the energy flow out of the HF stretching mode (from a time-dependent view) is very fast, occurring on a timescale of 2–20 ps.[19] In the absence of line resolution, it is not possible to quantify the timescale of predissociation. It could be as fast as 2–20 ps, but also considerably slower, when combined with IVR processes. However, it must be finite, as the band has been observed by monitoring the *depletion* of the mass spectrometer signal upon excitation.[19] The excess energy in an HF stretch excited $(HF)_3$ complex is so high that predissociation into three monomer fragments may occur in competition with the lower energy pathway involving a monomer and a dimer. There is some indirect experimental evidence for this triple fragmentation channel[19] in a low-temperature jet expansion, but theoretical calculations[35] indicate that the exothermicity is, at most, of the order of $100\,cm^{-1}$. Table 1 illustrates that in order to calculate such energy balances, three-body effects, anharmonicity in the HF stretching vibration, and anharmonic contributions to the zero-point energy have to be accurately included.

The latter involves knowledge of the global potential energy surface in 12 dimensions, not just the curvature at the minimum, and a technique to treat the nuclear quantum dynamics on this surface. Diffusion quantum Monte Carlo (DQMC) is among the few techniques which are capable of calculating anharmonic vibrational eigenstates in 12 (and more) dimensions. To understand qualitatively how it works, it is best to consider the origin of zero-point motion. It arises from Heisenberg's uncertainty relationship for location and momentum

$$\Delta x \Delta p \geq \hbar/2. \qquad (4)$$

In a potential well, a particle tries to optimize its energy within this constraint. It cannot sit in the minimum of the well ($\Delta x = \Delta p = 0$) like a classical particle. DQMC imposes a random motion on the particles, very much like the Brownian motion of an oil droplet in a water suspension. This random motion is constrained by a potential energy penalty such that the resulting trajectory exactly samples the ground-state wavefunction of the system (see reference 36 for more details and further references). Combined with an accurate pair potential[32] for HF and an *ab initio* based three-body potential,[35] DQMC allows the calculation of energy balances for predissociation, which are shown in Table 1.

For the fully deuterated isotopomer $(DF)_3$ these calculations make a surprising prediction. As a result of the lower stretching frequency of DF in $(DF)_3$ and the reduced zero point energy in the heavier molecular frame, both predissociation pathways are now energetically inaccessible. The dimer + monomer fragment channel is predicted at $\approx 35\,cm^{-1}$ above the DF stretching excitation, leaving IVR as the only way to redistribute vibrational energy. When one considers the remaining uncertainties in the pair and three-body potentials, such a prediction must be regarded as a suggestion/incentive for experimental verification. Stimulated by these calculations we investigated the DF stretching band at high resolution in a supersonic slit jet expansion using a difference frequency laser spectrometer;[24] the result is shown in Figure 4. Viewed at coarse grained level, it is a degenerate vibrational band of a planar symmetric top, as expected. The rotational constants are shown in Table 1 and are

Table 1 Comparison of experimental and theoretical results for $(HF)_3$ and $(DF)_3$ (all numbers except lifetimes (τ) in cm^{-1}). Experimental data are from reference 19 [$(HF)_3$, supersonic jet], reference 17 (matrix, $\tilde{\nu}_{FF}$), and reference 24 [$(DF)_3$, supersonic jet]. Theoretical results are based on the 1 + 2 + 3-body potential from reference 35 combined with quantum Monte Carlo and grid calculations. Results obtained by neglecting the three-body contribution are given in parentheses. Rotational constants are evaluated at the planar minimum (C_e) and including zero-point averaging effects (C_0). Electronic well depths (D_e) and harmonic (D_0^h) as well as anharmonic binding energies (D_0) are expressed relative to the dimer + monomer dissociation limit ([2 + 1]) and relative to the three monomer limit ([1 + 1 + 1]). IR-active HF stretching wavenumbers and wavenumber shifts relative to the monomer (Δ) as well as FF stretching wavenumbers are evaluated harmonically [$(\Delta)\omega$] and anharmonically [$\Delta)\tilde{\nu}$].

	$(HF)_3$		$(DF)_3$	
	exp.	theor.	exp.	theor.
$C_0 \approx B_0/2$		0.124	0.120	0.121 (0.107)
$C_e = B_e/2$		0.129		0.125
$D_0[2+1]/hc$	$\leq 2650^a$	2561 (1951)	≥ 2725	2768 (2115)
$D_0^h[2+1]/hc$		2494		2726
$D_0[1+1+1]/hc$	$\leq 3712^a$	3623	≥ 3894	3933
$D_e[2+1]/hc$		3524		3524
$\tau_{IVR/PD}$/ps	2–20		40	
τ_{PD}/ps	>2–20 $<\infty$		>3000	
$\tilde{\nu}_{HF}$	3712	3716	2724.6	2733
$\Delta\tilde{\nu}_{HF}$	-249	-245	-182.1	-173
ω_{HF}		3912		2836
$\Delta\omega_{HF}$		-221 (-108)		-161 (-79)
$\tilde{\nu}_{FF}$	152.5	153	155.5	155
ω_{FF}		180 (129)		174 (126)

[a] Most probable interpretation of the experimental data.

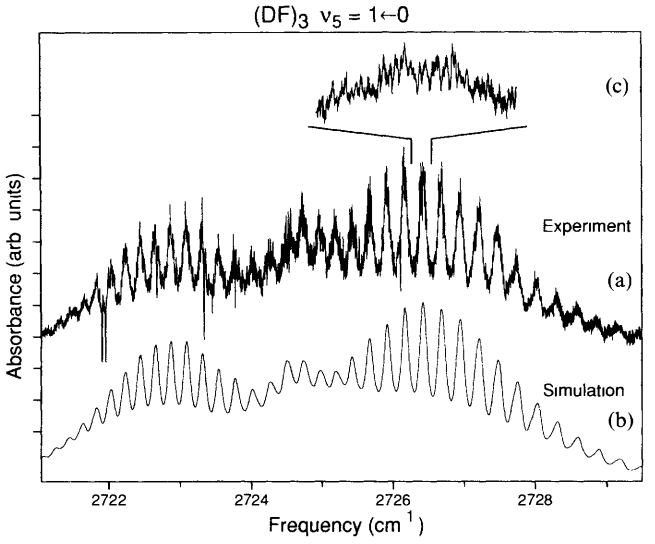

Figure 4 (a) Near IR survey spectrum over ν_5 of $(DF)_3$ displaying a clear perpendicular band characteristic of a planar (or near planar) oblate symmetric top The few sharp downward going signals are due to HDO traces in the vacuum chamber and conveniently serve as a frequency calibration (b) Simulation of the $(DF)_3$ spectrum modelled as a perpendicular band of an oblate symmetric top at 10 3 K but with each transition broadened by a uniform Lorentzian line width of $\gamma = 0\ 133\ cm^{-1}$ The rotational constants from this fit are in remark ably good agreement with the QMC predictions on the Quack and Suhm potential energy surface for the trimer (c) The sharp fine structure (see inset) in the spectrum is quite real due to IVR coupling of the initial ν_5 excitation into the bath modes of the cyclic ring and causing the ring to break open on the 40 ps time scale

seen to be consistent with predictions from the potential energy surface, which features an FF-distance of 258pm and a hydrogen bond angle 24° at equilibrium

At higher resolution, however, the appearance of the spectrum is inconsistent with an isolated absorption band at 10 K Specifically, there are as much as 1000-fold more lines than expected, and one has to invoke extensive coupling to other states *via* intramolecular vibrational redistribution (IVR) The resulting spectrum appears to be described well by a simple Lorentzian line shape for each zero-order transition, indicating a dense manifold of coupling states and more or less statistical coupling In this statistical limit, one can use equation 3 and infer a lifetime of 40 ps for the DF stretching vibration in the time-dependent picture So far, the situation is quite similar to the $(HF)_3$ case, with the sole difference that the increased lifetime allows for the extraction of a geometry How can we verify the prediction that the decay of the stretching state is due to IVR, but *not* to predissociation? From DQMC calculations in the potential surface, the density of ro-vibrational states at the excitation frequency can be calculated If we assume the extreme case that all available states (within the rigorous constraints of symmetry and total angular momentum) can couple to the DF stretching state, and if we further assume that the distribution of the coupled states obeys the most probable distribution law,[24] there should still be line structure visible within the Lorentzian humps at the Doppler-limited resolution of 40 MHz Figure 4 shows that there is in fact narrow line structure in the spectrum at this resolution Closer examination shows no sign of additional predissociation broadening in the lines beyond the 40 MHz experimental apparatus limit, although the congested nature of the spectrum only allows rigorous exclusion of lifetimes below 3 ns for some of the transitions Any significant excitation above threshold in such a strongly coupled system should lead to much shorter lifetimes [24] The conclusion is therefore that this band is most likely below the predissociation threshold Stochastic simulation of the spectrum (Figure 4)[24] shows that the extreme assumption of coupling to virtually all excited states (about $200(2J + 1)/cm^{-1}$, where J is the rotational quantum number) is necessary to explain the dense structure

From linear combinations of these dense eigenstates, the DF stretching band tells an equivalent story about the evolution of jet-cooled $(DF)_3$ in the time domain subsequent to excitation by a coherent sub-picosecond laser pulse centred at $2725\ cm^{-1}$ All the energy is initially put into the DF stretching coordinate, where it excites an oscillation with 0 012 ps period On a time scale of 40 ps, this energy flows into other degrees of freedom Without detailed analysis of the spectra, we cannot say whether this flow occurs in a sequential manner through some specific, so-called doorway states, or whether the process is more statistical [26 29] Upon completion of this energy redistribution, the clusters are in a vibrationally very hot state, on the order of 5% below dissociation threshold, whereas rotationally they are as cold as before, J being conserved For a given J, practically all energetically accessible states are populated For statistical reasons, a vast majority of these states will have largest amplitude in open-chain configurations Effectively, this means that the ring has 'cracked open' on a 40 ps timescale, although on the average, the remaining two hydrogen bonds will also be severely stretched After completion of this redistribution, the energy keeps rattling around in the molecule, but nothing new happens until the clusters collide or radiate This is a nice example of the dynamical information which can be extracted from a stochastic spectrum in the absence of any time-resolved experiment

For a second example of $(HF)_3$ *vs* $(DF)_3$ dynamics, we consider hydrogen bond stretching motion The masses involved in this motion are an order of magnitude larger, and the 'springs' connecting the vibrating bodies are two orders of magnitude smaller This means that we have to move to the FIR range, around 150 cm^{-1} Reference 14 shows a survey of the FIR spectrum of HF vapour around this range The weak $(HF)_3$ hydrogen bond stretching band is well hidden underneath strong monomer rotational transitions, dimer librational and rotational bands, and a broad structureless band due to hydrogen bond stretching in larger clusters Therefore, a gas phase assignment of the trimer band is still missing By isolating $(HF)_3$ in rare gas matrices,[17] the complicated rotational structure is removed at the price of inducing small frequency shifts due to interaction with the matrix In fact, one is effectively studying clusters $(HF)_3(Rg)_\infty$ (Rg = Ar,Ne) This makes absolute correlations between gas phase and matrix difficult, but here we want to concentrate on a relative effect between different isotopomers, where matrix data can be more reliable It was observed that the hydrogen bond stretching band in $(DF)_3$ ($155\ 5\ cm^{-1}$) occurs at a *higher* frequency than that of $(HF)_3$ ($152\ 5\ cm^{-1}$) This contradicts the simple one-dimensional oscillator formula

$$\nu = \frac{1}{2\pi}\sqrt{\frac{f}{\mu}} \tag{5}$$

which predicts a frequency decrease with increasing mass μ, given the same force constant f One is forced to conclude that the force constant, *i e* the vibrational potential, must be different for $(HF)_3$ and $(DF)_3$ Within the Born–Oppenheimer separation of electronic and nuclear motion, this should not be the case and it is highly unlikely that a breakdown of this separation is observed in this case In fact, the explanation is much simpler – we are looking at a one-dimensional hydrogen bond stretching motion (actually it is two-dimensional, because the IR-active vibration is degenerate, but this does not change the conclusion[35]) As pointed out in Section 4 2, motion in the remaining 10 dimensions has the effect of distorting this electronic 1-D potential to an effective adiabatic potential, which is the relevant potential for stretching motion This distortion is mass dependent, as it is caused by the zero-point energy in the remaining dimensions For $(HF)_3$, zero-point energy effects are larger than for $(DF)_3$, making the effective stretching potential more shallow and hence lowering the frequency (*cf* Figure 3) In order to see whether this qualitative explanation accounts for the

observed effect in a quantitative way, we have carried out DQMC calculations,[35] in which the stretching motion was forced on the one-dimensional path, whereas the remaining coordinates were allowed to vibrate freely. Table 1 shows the results, which are in excellent agreement with the matrix data,[17] when anharmonic zero-point motion effects are taken into account. While the absolute agreement must in part be fortuitous, given the uncertainties associated with both the experiment and potential energy surface, the prediction of an inverse isotope effect of the right order of magnitude is rewarding and confirms the accuracy of the three-body potential. Some of the librational bands which are responsible for this peculiar effect have also been probed directly using a CO_2 laser.[34]

These selected dynamical phenomena in $(HF)_3$ serve to illustrate the power of IR spectroscopy in studying hydrogen bonding and in revealing large three-body effects. We will now turn to weaker interactions, where the three-body forces are more subtle.

6 $Ar(HF)_2$ – Lack of Experimental Evidence

In view of the great diversity of trimers which have been studied experimentally and by theoretical methods, it is very surprising that no analysed spectroscopic data appear to exist for $Ar(HF)_2$.[37] Since the Ar–HF[31] and HF–HF[32] pair potentials are among the best known, a pairwise additive potential surface can immediately be constructed and investigated. Such a pairwise additive approach should be quite reasonable as an initial guess. Of course, a full treatment of the vibrational dynamics is formidable, but intelligent approximations can be made.

Considering the relative bond strengths of ArHF and $(HF)_2$, it is probably best to view $Ar(HF)_2$ as an Ar atom attached to HF dimer. The vibrational frequency shifts induced by this attachment can be estimated from the shifts observed for $(HF)_2$ in Ar matrix, which are known to be quite small in many cases.[17] It is beyond the scope of this article to make detailed predictions on the vibrational spectra of $Ar(HF)_2$, but forthcoming experimental and theoretical progress may be safely anticipated in this arena.

7 Pairwise and Non-additive Effects in Ar_2HF

As we proceed along this series of $Ar_n(HF)_{3-n}$ trimers, the study of Ar_2HF and Ar_2DF takes on a special significance. First of all, quantitatively reliable pairwise additive potentials for the rare gas–HX systems are now available, both as a function of inter- and intramolecular coordinates.[38] Secondly, the rare gas–rare gas potentials have been well studied in crossed beam studies, and in some cases such as Ar–Ar, also from spectroscopic investigations of the rare gas excimer dimers.[20,39] Thus, one can easily imagine constructing a potential for HF 'solvated' in an arbitrarily large cluster of Ar. Since the corresponding kinetic energy terms in the Hamiltonian are well understood, in principle we should have a completely predictive understanding of these species, at the pairwise additive level. Experiment, of course, cannot neglect additional three-body interactions, and will yield results close to but subtly different from prediction. The interesting challenge, clearly, is to exploit high resolution spectroscopy in these small trimer clusters as a nearly ideal 'microcanonical' laboratory for three body forces.[8,21,37,40]

As a zero-order test, we can predict the equilibrium structures from the pairwise additive potentials for the series of Ar_n–HF and Ar_n–DF clusters as a function of $n = 1,2,3,\ldots$. The predicted structures are shown in Figure 5; the numbers indicate the potential minimum (in cm^{-1}) with respect to the asymptotic separation of the monomer subunits. Interestingly, the lowest energy structures correspond to preferential clustering around the H end of the molecule, rather than uniform 'solvation' of the HF subunit (see for example the lowest $n = 3$ *vs.* $n = 4$ structure). In all cases, the structures are in good agreement with the species observed in FT microwave and near-IR supersonic jet spectra.[21,37]

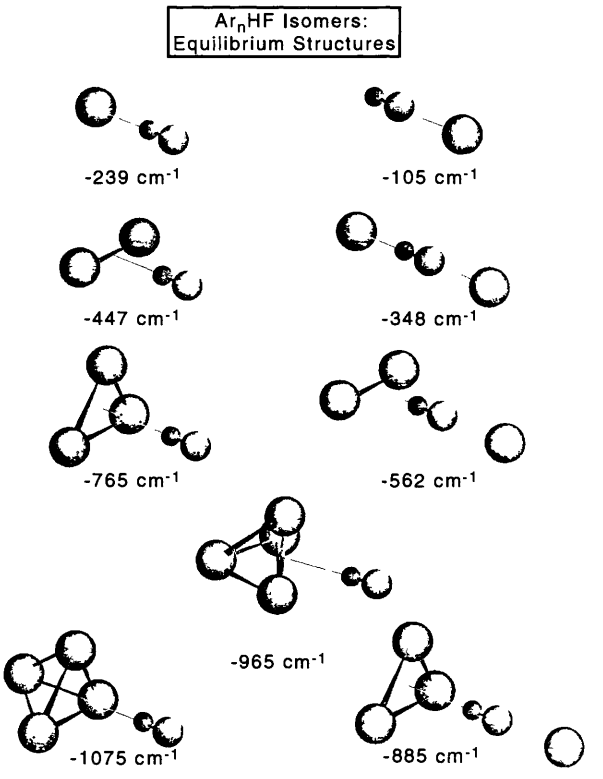

Figure 5 Equilibrium structures for Ar_nHF and Ar_nDF isomers, predicted from pairwise additive potentials for Ar–HF and Ar–Ar. The energies of each structure are with respect to the fully separated (n)Ar + HF monomer species. Note the lowest energy isomer predicts the $(Ar)_n$ bonds preferentially on the H end of HF, in agreement with experimental observation. Note also the existence of several nearly isoenergetic isomers for the $n = 4$ species; for $n > 4$, the number of such multiple minima grows dramatically.

A more quantitative probe of the three-body effects, however, can be obtained directly from studies of the low frequency van der Waals modes themselves, particularly those arising from HX bending motion which acquire reasonable oscillator strengths. We have recently observed[41] and assigned the two strongest intermolecular bands in Ar_2HF and Ar_2DF complexes, corresponding to the HF 'in-plane' and 'out-of-plane' bend. The results, along with the theoretical predictions for a pure pairwise additive potential surface, are presented in Figure 6. Note the systematic overestimation of all the bend frequencies, and thus that the additive potentials overestimate the angular anisotropy felt by the HF (or DF) in the presence of Ar–Ar. This effect has been elegantly elucidated by Hutson and co-workers.[8] It appears to be predominantly attributable to 'Pauli exclusion principle' formation of a quadrupole on the Ar–Ar due to overlap repulsion of the electron clouds. This generates additional 'exchange multipole' terms, which, sampled at close range by the HF dipole, significantly decrease the angular anisotropy as experimentally observed. In simple terms, the pairwise-additive compromise position of the HF dipole vector (*i.e.*, pointing exactly midway between the two Ar atoms) becomes less attractive, because this happens to be the zone of maximum Pauli exclusion. Hence, the three-body effect makes it easier to bend the HF out of the symmetric position and there is even speculation that the bending motion initially goes slightly downhill.[42] Such subtle details of the potential energy surface are quite hard to identify spectroscopically or by any other method. It is interesting to note that the three-body exchange multipole effects in Ar_2HF are in fact more than five-fold stronger than the conventional Axilrod–Teller three-body terms, and thus ironically dominate the non-pairwise behaviour in HX/rare gas systems.

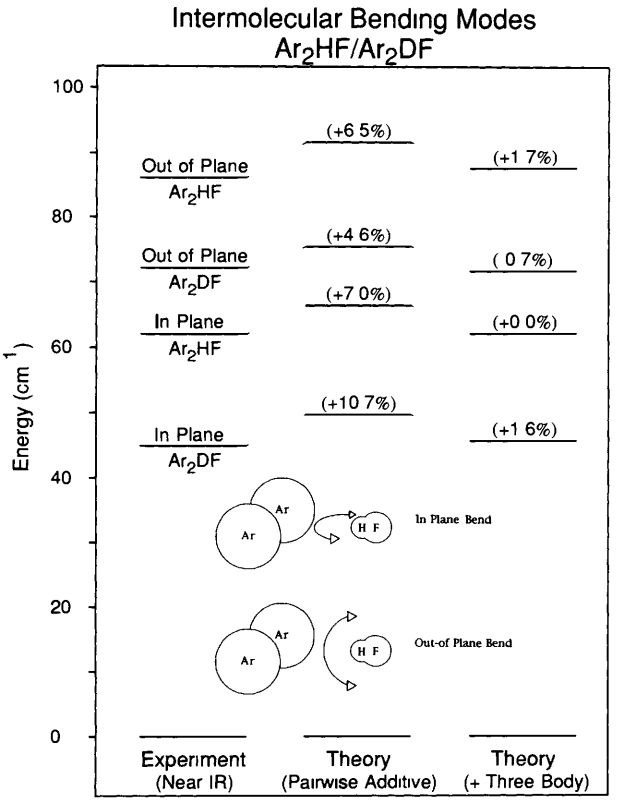

Figure 6 Intermolecular 'in-plane and out-of plane' bending vibrations in Ar_2HF and Ar_2DF The left column indicates the experimentally observed values, the middle column represents close-coupled QM predictions on the pure pairwise additive potential surface (% error values in parentheses) Note the systematic *overprediction* of these bending frequencies, *i e* , the bend anisotropy is too strong Addition of the lowest order three-body terms (Axilrod–Teller, triple dipole, and Pauli exchange repulsion) significantly reduces this anisotropy, bringing prediction into much better agreement with experiment It is worth noting that conventional Axilrod–Teller contributions are quite small (<20%), and that the Pauli exchange terms account for more than 70% of the observed three-body effects

8 Ar_3 – Does it Have an IR Spectrum?

The Ar trimer differs substantially from the other trimers in the series, as it does not contain any polar constituents One might doubt whether IR spectroscopy can contribute at all to our understanding of this complex In fact, no IR absorptions have been detected so far and it is quite possible that Raman or electronic[20] spectroscopy will be more successful in characterizing it However, in one aspect the IR spectrum of Ar clusters differs uniquely from the other members of the Ar–HF series *Any* IR absorption (of electric dipole type) found *must* be due to trimers or larger clusters, as binary collisions of two Ar atoms by symmetry cannot even create a temporary dipole moment Ternary collisions may well produce such a temporary dipole moment and the resulting collision-induced FIR spectra are the subject of some theoretical investigations [43] The lowest mode with non-zero IR activity (comparable in strength to the 4th overtone of the HF stretching vibration[44]) is predicted near 22 5 cm^{-1} (the asymmetric Ar–Ar stretch) Given a potential energy and dipole surface, such predictions are relatively easy to make for Ar_3, as only three vibrational degrees of freedom are involved Three-body contributions to the Ar interaction potential are very subtle and appear to involve substantial cancellation between different mechanisms [7] Current estimates of these three-body effects are on the order of 1% of the relevant IR transition frequencies [44] Nevertheless, the extremely accurate pair potentials available for Ar,[39] obtained mostly through non-spectroscopic techniques, justifies the current search for these subtle non-additive effects Of course, since the origin of *any* dipole oscillator strength for such transitions arises purely from non-pairwise additive contributions, measurement of the absolute absorption strengths would reflect effects 100% due to three-body interactions Though experimentally challenging, this offers a significant advantage over the process described above, which relies on quantitative accuracy of pairwise contributions to infer small differences between prediction and experiment

9 Towards Bulk Properties

In view of the effort associated with a detailed characterization of three-body forces in intermolecular interactions, the aim of understanding condensed phases through a spectroscopic cluster approach with *n*-body potential contributions may seem quite remote Fortunately, this is a misleading impression In fact, evidence for the relative insignificance of higher than two- and three-body contributions is growing [21 25 33 35 45] Naturally, there will be exceptions to this rule Very subtle effects such as the relative energy of hexagonal and cubic close packings of rare-gas solids are thought to depend on truly many-body terms ($n > 3$) caused by crystal field effects [11] Covalently bound species such as C_{60} have also been treated in the context of pairwise and non-pairwise additive atom–atom interactions However, since these 'clusters' are not formed from closed-shell constituents, there may also be sizeable higher-body contributions to the potential energy function

For the important classes of van der Waals and hydrogen bond interactions, however, a compact 1 + 2 + 3-body approach should be able to provide a satisfactory description of arbitrarily sized clusters and bulk matter, including solvent effects [28] The programme ahead of us is therefore quite clear spectroscopic characterization of all dimers *and* trimers composed of the monomers which are of interest, supported and complemented by theoretical calculations of the corresponding potential hypersurfaces Accurate treatment of the nuclear quantum dynamics forms the crucial link between the spectra and their associated potentials For binary complexes, this programme is making excellent progress in ours and many other laboratories, and is already rather complete for selected molecules For trimers, we have exemplified that it is feasible by highlighting a few examples from others and our own work, but a lot of systematic work remains to be done

Acknowledgment DJN would like to acknowledge support from the National Science Foundation for this work, and to Dr Jeremy Hutson and John Farrell for helpful discussions MAS thanks Professor Martin Quack for support and many insights about how to relate potentials, spectra, and dynamics, Dr Jurgen Stohner and Dr David Luckhaus for helpful discussions, the Deutsche Forschungsgemeinschaft for a scholarship and the Rechenzentrum der ETH as well as the CSCS for generous computer grants

10 References

1 The nomenclature for molecular aggregates is not uniform The names 'dimer', 'trimer', 'oligomer', and 'polymer' are sometimes restricted to identical subunits, despite the Greek word *meros* = part, which suggests nothing about the identity of the parts We prefer to use 'trimer' in its literal (and often used) meaning for any aggregate formed by three constituents If one wants to be more specific, a prefix can be added, 'homo-', 'hetero-', 'co-' are in use, more detailed prefixes such as '[2,1]-' or the chemical formula can always be specified

2 T R Dyke, B J Howard, and W Klemperer, *J Chem Phys* , 1972, **56**, 2442–2454

3 C M Lovejoy, M D Schuder, and D J Nesbitt, *J Chem Phys* , 1986, **85**, 4890–4902

4 D J Nesbitt, *Chem Rev* , 1988, **88**, 843–870

5 R E Miller, *Adv Mol Vib Collision Dyn* , 1992, **1A**, 83–108

6 P Schuster, *Angew Chem Int Ed Engl* , 1981, **20**, 546–568

7 M M Szczęsniak and G Chałasinski, *J Mol Struct (THEOCHEM)*, 1992, **261**, 37–54

8 A R Cooper and J M Hutson, *J Chem Phys*, 1993, **98**, 5337–5351
9 B M Axilrod and E Teller, *J Chem Phys*, 1943, **11**, 299–300
10 G Chałasinski, S M Cybulski, M M Szczęsniak, and S Scheiner, *J Chem Phys*, 1989, **91**, 7048–7056
11 K F Niebel and J A Venables, in 'Rare Gas Solids', Vol 1, ed M L Klein and J A Venables, Academic Press, London, 1976, pp 558–589
12 M A Suhm, *Chem Phys Lett*, 1994, **223**, 474–480
13 N Moazzen-Ahmadi, A R W McKellar, and J W C Johns, *Chem Phys Lett*, 1988, **151**, 318–322
14 M Quack and M A Suhm, *Chem Phys Lett*, 1990, **171**, 517–524
15 R J Saykally, *Acc Chem Res*, 1989, **22**, 295–300
16 K v Puttkamer and M Quack, *Mol Phys*, 1987, **62**, 1047–1064
17 L Andrews, S R Davis, and R D Hunt, 1992, *Mol Phys*, **77**, 993–1003
18 A S Pine, W J Lafferty, and B J Howard, *J Chem Phys*, 1984, **81**, 2939–2950
19 D W Michael and J M Lisy, *J Chem Phys*, 1986, **85**, 2528–2537
20 P R Herman, P E LaRocque, and B P Stoicheff, *J Chem Phys*, 1988, **89**, 4535–4549
21 A McIlroy, R Lascola, C M Lovejoy, and D J Nesbitt, *J Phys Chem*, 1991, **95**, 2636–2644
22 N Pugliano and R J Saykally, *Science*, 1992, **257**, 1937–1940
23 U Buck, *Ber Bunsenges Phys Chem*, 1992, **96**, 1275–1284
24 M A Suhm, J T Farrell, Jr, S Ashworth, and D J Nesbitt, *J Chem Phys*, 1993, **98**, 5985–5989, J Han, Z Wang, A L McIntosh, R R Lucchese, and J W Bevan, *J Chem Phys*, 1994, **100**, 7101–7108
25 M Quack, U Schmitt, and M A Suhm, *Chem Phys Lett*, 1993, **208**, 446–452
26 D J Nesbitt, in 'Reaction Dynamics in Clusters and Condensed Phases', Vol 26, ed J Jortner, R D Levine, and B Pullman, Kluwer, 1994, pp 137–151
27 S Coussan, N Bakkas, A Loutellier, J P Perchard, and S Racine, *Chem Phys Lett*, 1994, **217**, 123–130
28 A D Buckingham, *Proc R Soc London Ser A*, 1958, **248**, 169–182
29 K v Puttkamer and M Quack, *Chem Phys*, 1989, **139**, 31–53
30 M A Suhm, J T Farrell, Jr, A McIlroy, and D J Nesbitt, *J Chem Phys*, 1992, **97**, 5341–5354
31 H -C Chang, F -M Tao, and W Klemperer, *J Chem Phys*, 1993, **99**, 9337–9349
32 M Quack and M A Suhm, *J Chem Phys*, 1991, **95**, 28–59
33 A McIlroy and D J Nesbitt, *J Chem Phys*, 1992, **97**, 6044–6056
34 K D Kolenbrander, C E Dykstra, and J M Lisy, *J Chem Phys*, 1988, **88**, 5995–6012
35 M Quack, J Stohner, and M A Suhm, *J Mol Struct*, 1993, **294**, 33–36, and to be published
36 M A Suhm and R O Watts, *Physics Reports*, 1991, **204**, 293–329
37 H S Gutowsky, T D Klots, C Chuang, J D Keen, C A Schmuttenmaer, and T Emilsson, *J Am Chem Soc*, 1985, **107**, 7174–7175
38 J M Hutson, *J Chem Phys*, 1992, **96**, 6752–6767
39 R A Aziz, *J Chem Phys*, 1993, **99**, 4518–4525
40 M J Elrod, J G Loeser, and R J Saykally, *J Chem Phys*, 1993, **98**, 5352–5361
41 J T Farrell, Jr and D J Nesbitt, manuscript in preparation
42 M M Szczęsniak, G Chałasinski, and P Piecuch, *J Chem Phys*, 1993, **99**, 6732–6741
43 B Guillot, R D Mountain, and G Birnbaum, *Mol Phys*, 1988, **64**, 747–757
44 A R Cooper, S Jain, and J M Hutson, *J Chem Phys*, 1993, **98**, 2160–2169
45 S Green and J Hutson, *J Chem Phys*, 1994, **100**, 891–898